Raman and infrared measurements on the $[Mn_4]_2$ dimer: A single-molecule magnet with an exchange bias

J. M. North and N. S. Dalal
Department of Chemistry and Biochemistry and National High Magnetic Field Laboratory, Florida State University, Tallahassee, Florida 32306, USA

D. Foguet-Albiol, A. Vinslava, and G. Christou
Department of Chemistry, University of Florida, Gainesville, Florida 32611, USA
(Received 3 December 2003; published 20 May 2004)

We report Raman and infrared (IR) absorption measurements on the dimeric single-molecule magnet $[Mn_4O_3Cl_4(O_2CEt)_3(py)_3]_2$, (Et=ethyl, C_2H_5; py=pyridine, C_5H_5N) to complement the recent density-functional calculations on this unusual material. The Raman data fall essentially under four categories. With the theoretically predicted values in parentheses, they are (a) peaks at 192 (194), 219 (212), and 274 (278) cm^{-1} which are assignable to metal-ligand vibrations not involving the O^{2-} moieties, (b) peaks at 316 (301), 354 (361), 382 (380), 409 (423), 443 (444), 509 (514), 537 (543), and 608 (602) cm^{-1} assigned to Mn-O vibrations, (c) peaks at 647 (640) and 1017 (1019), 1075 (1066), 1160, 1222 (1207), 1541 (1547), 1570 (1563), and 1609 (1604) cm^{-1} matching with pyridine vibrations, and (d) modes at 1044, 1399, 1541 (1547), 1570 (1563), and 1609 (1604) cm^{-1}, which are attributed to vibrations in O_2CEt groups. Several peaks not predicted by the density-functional theory calculations are assigned using spectra of model compounds. IR spectra, which are reported from 400–4000 cm^{-1}, match reasonably well with the Raman spectra. Furthermore, many of the theoretically predicted Raman and IR peak positions compare reasonably well with the experimental spectra, but the origin of a few others remains unclear.

DOI: 10.1103/PhysRevB.69.174419 PACS number(s): 75.50.−y, 78.20.−e, 78.30.−j

I. INTRODUCTION

Single-molecule magnets, SMM's, consisting of a monodisperse array of transition-metal ions bound by organic ligands, have been of high theoretical and experimental interest lately due to their unique magnetic properties, such as the ability of a single molecule to exhibit magnetic hysteresis.[1,2] This unique domain effect of a single molecule may potentially lead to the development of the ultimate high-density magnetic memory devices[1,2] and quantum computation.[3] The most thoroughly characterized SMM's are $[Mn_{12}O_{12}(O_2CMe)_{16}(H_2O)_4]\cdot 2O_2CMe\cdot 4H_2O$ (Mn_{12}-acetate),[4] $[(C_6H_{15}N_3)_6Fe_8(\mu_3\text{-}O)_2(\mu_2\text{-}OH)_{12}]Br_7(H_2O)Br\cdot 8H_2O$ (Fe_8Br_8),[5] and the $[Mn_4O_3Cl_4(O_2CR)_3(py)_3]$ (py=pyridine, C_2H_5N) family (Mn_4),[6,7] all exhibiting the unique property of macroscopic quantum tunneling (MQT) which manifests itself in the temperature independence of the magnetic relaxation data, and as quantized steps in the magnetic hysteresis loops.[8–11] It should also be mentioned that pure quantum tunneling in Mn_{12}-acetate was first observed by Bokacheva *et al.*[12]

Wernsdorfer *et al.*[13] have reported studies on a related class of SMM's consisting of dimeric units, which exhibit a new behavior in the quantized steps: the absence of a step at zero field. The first member of this series to be studied was $[Mn_4O_3Cl_4(O_2CEt)_3(py)_3]_2$ (Et=ethyl, C_2H_5; py=pyridine, C_5H_5N), abbreviated $[Mn_4]_2$, whose structure is shown in Fig. 1. This was quite a significant development because the presence of a step at zero magnetic field implies that such a compound will always need a magnetic field to control the leakage of magnetization, and hence to prevent the loss of stored information from such a memory element. With this lack of a step at zero field, the dimerized $[Mn_4]_2$ compound alleviates potential memory loss problems which would be present in all previously characterized SMM's. Very recently Hill *et al.*[14] have demonstrated quantum coherence in the same system, which opens new avenues for quantum computation.

The $[Mn_4]_2$ system consists of dimerized cubane structures, which are well isolated from neighboring pairs. Each of the cubanes contains three Mn^{3+} ($S=2$) and one Mn^{4+} ($S=3/2$) joined together by three oxygens and one chlorine serving as vertices. The three Mn^{3+} are coupled antiferromagnetically to Mn^{4+}, yielding a total spin of $S=(3\times 2)-3/2=9/2$. The dimers are held together by six C-H$\cdots$Cl hydrogen bonds between the pyridine rings of one Mn_4 to the Cl ions of the other. The hydrogen bond distances are about 3.71 Å, which is typical for this type of bond. Additionally, the central bridging Cl ions for each Mn_4 cube are in close proximity to one another, separated by only about 3.858 Å.[13]

In an effort to understand the lack of a step at zero field, Park *et al.*[15,16] have reported on a detailed electronic structure calculation of this system, using the density-functional theory (DFT). In particular, they have predicted the vibrational energy levels, positions, and intensities of the IR and Raman peaks. Earlier, Pederson *et al.*[17] had suggested that some of the spin-vibron interactions might play a role in the mechanism of MQT in Mn_{12}-acetate and related SMM's. They also predicted the positions of several such low-lying vibrational modes. Recent IR (Refs. 18–21) and Raman[20–22] measurements have confirmed the mode predictions.[17] With

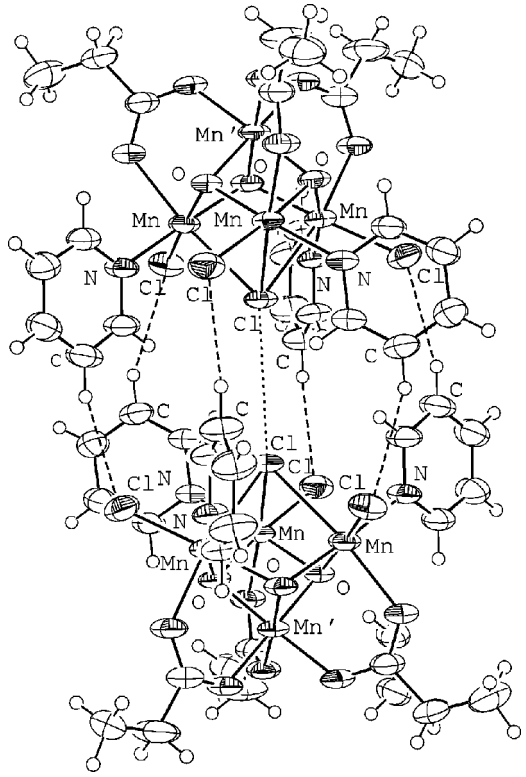

FIG. 1. The crystal structure of the $[Mn_4]_2$ dimer showing the six C-H$\cdots$Cl bonds (dashed lines), which connect the monomers (Ref. 13). The dotted line is the close approach of the central Cl atoms, and thus probably the main superexchange pathway.

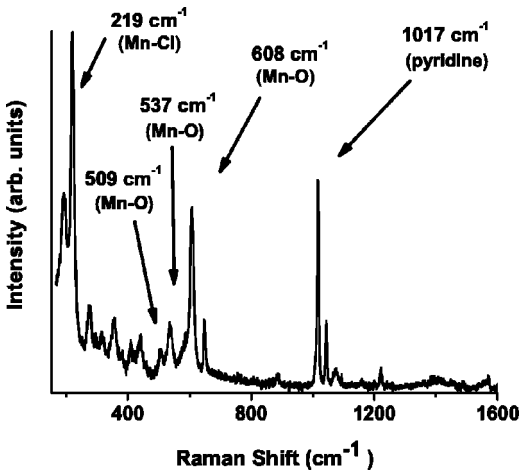

FIG. 2. The Raman modes of $[Mn_4]_2$. The marked peaks correspond to a few modes predicted by theoretical calculations (Ref. 15).

these results in mind, we now report on an IR and Raman study of $[Mn_4]_2$. Peak assignments have been made using the model compounds MnO_2, $KMnO_4$, $Mn(O_2CMe)_2$, and $MnCl_2$. Additionally, the spectrum of $[Mn_4]_2$ is compared to spectra of the monomeric compounds $Mn_4O_3Cl(O_2CEt)_3(dbm)_3$ (abbreviated Mn_4-Pr) and $Mn_4O_3Cl(O_2CMe)_3(dbm)_3$ (abbreviated Mn_4-Ac). These compounds contain the identical core cubane structure of $[Mn_4]_2$, but differ in some of the ligands attached. Our data show good agreement with many of the theoretically predicted peaks, but there are several additional ones, whose origin still remains unclear.

Section II describes the experimental details of the Raman and IR spectrometers. The results are presented in Sec. III, together with their interpretation using the model compounds and the theoretical results of Park *et al.*[15] with the conclusions summarized in Sec. IV.

II. EXPERIMENT

Sample preparation: All manipulations were performed under anaerobic conditions using distilled solvents. All reagents were used as received. The complexes $[Mn_3O(O_2CMe)_6(py)_3](ClO_4)$ and $[Mn_4O_3Cl_4(O_2CEt)_3(py)_3]_2$, ($[Mn_4]_2$), were prepared as described in Refs. 23 and 24, respectively.

Raman and IR measurements: Raman spectra were obtained using a JY Horiba LabRam HR800 microRaman spectrograph at room temperature. An 80 mW laser emitting at 785 nm was used as the excitation source. Care was taken to minimize laser damage to the sample as previously discussed.[20–22] A 50 X 0.10 NA (numerical aperture) objective with exposure times of 60 s averaged through ten scans was found to be sufficient for obtaining a reasonably strong spectrum. IR measurements were collected as KBr disks at room temperature on a Nicolet model 510 P spectrophotometer.

III. RESULTS

Figure 2 shows a typical Raman spectrum of the SMM $[Mn_4]_2$. Numerous strong peaks can be seen below 1600 cm^{-1}. Their positions (in centimeter inverse units) are collected in Table I. As discussed by Park *et al.*[15] most of the vibrational data can be analyzed roughly within the harmonic-oscillator approximation by using the monomer as a model, and replacing the CH_2CH_3 group by H. There are a total of $3N=3\times56=168$ degrees of freedom, six of which are translational and rotational modes. All the others were considered vibrationally stable. The observed Raman peaks can be broadly lumped into four groups, following the DFT results[15] as summarized below.

A. Peak assignment from DFT calculations

a. Metal-ligand vibrations not involving O^{2-}. The peaks observed experimentally at 192, 219, and 274 cm^{-1} are predicted in the DFT calculations[15] at 194, 212, and 278 cm^{-1}, respectively. They are attributed to contributions from all components in the system, with the exception of O^{2-}.

b. Mn-O vibrations. Modes which are predicted at 301, 361, 380, 423, 444, 514, 543, and 602 cm^{-1}, and seen in the Raman data at 316, 354, 382, 409, 443, 509, 537, and 608 cm^{-1}, respectively, are assigned to contributions from the O^{2-} and Mn atoms only.

c. Pyridine vibrations. The peak observed experimentally at 647 cm^{-1} is predicted in the theory at 640 cm^{-1}.[15] A very

TABLE I. Raman and IR modes (cm^{-1}) and DFT calculations (Ref. 15) of vibrational modes for $[Mn_4]_2$ at 295 K. Theoretical calculation of Raman modes are denoted with R and IR modes with I. Assignments by experiment are denoted with Ex and those by theory with T.

$[Mn_4]_2$ Raman modes	$[Mn_4]_2$ IR modes	Theory (Ref. 15)	Assignment
		168 (R,I)	All components except O^{2-} (T)
192		194 (R,I)	Mn-Cl (cubane) (Ex), all components except O^{2-} (T)
219		211 (I), 212 (R)	All components except O^{2-} (T)
		247 (R)	All components (T)
		259 (R,I)	All components (T)
274		277 (I), 278(R)	Mn-Cl (ligand) (Ex), all components (T)
316		301 (R,I)	Mn-O (Ex), all components (T)
354		361 (R,I)	Mn-O (Ex), all components (T)
382		380 (R,I)	Mn-O_2CEt (T)
409		423 (R), 425 (I)	Mn-O (Ex), all components (T)
443	438	444 (R,I)	Mn-O_2CEt (Ex,T)
		491 (R,I)	Mn-O (T)
509	508	514 (R,I)	Mn-O (Ex,T)
537	539	543 (R,I)	Mn-O (T)
588	587		
608	608	602 (R,I)	Mn-O (T)
647	649	640 (R)	Pyridine (Ex,T)
	694	671 (R,I)	Pyridine (T)
	767	745 (R,I)	O_2CH, pyridine (T)
810	814		
		844 (R,I)	Pyridine (T)
	886		
	918	920 (R)	Mn-O (Ex), pyridine (T)
		955 (R,I)	Pyridine (T)
		977 (I)	Pyridine (T)
		991 (R,I)	O_2CH, pyridine (T)
1017	1016	1019 (R,I)	Pyridine (T)
1044	1044		O_2CEt (Ex)
1075	1073	1066 (R,I)	Pyridine (T)
1160	1161		Pyridine (Ex)
1222	1221	1207 (R)	Pyridine (T)
	1290		
		1316 (R,I)	O_2CEt, pyridine (T)
		1339 (R)	O_2CEt, pyridine (T)
	1370		
1399	1399		O_2CEt, Mn-O-R (Ex)
	1450	1439 (R,I)	Pyridine (T)
	1488	1472 (R,I)	Pyridine (T)
1541	1547	1547 (R,I)	O_2CEt, pyridine, Mn-O-R (Ex,T)
1570	1565	1563 (R,I)	O_2CEt, pyridine, Mn-O-R (Ex,T)
1609	1608	1604 (R,I)	O_2CEt, pyridine, Mn-O-R (Ex,T)
	2941	2942 (R,I)	O_2CEt, pyridine (Ex,T) (symmetric C-H) (Ref. 25)
	2980		O_2CEt, pyridine (Ex,T) (asymmetric C-H) (Ref. 25)
		3115 (R,I)	Pyridine (T)
		3132 (R)	Pyridine (T)
		3154 (R,I)	Pyridine (T)
	3416		Background

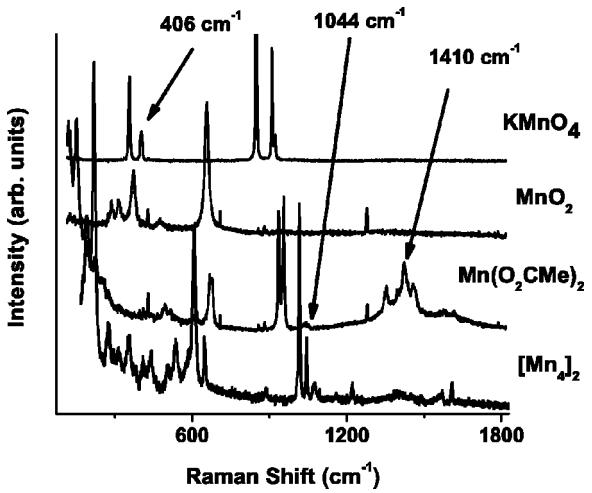

FIG. 3. Comparison of the Raman spectra of model compounds to that of $[Mn_4]_2$ at 295 K.

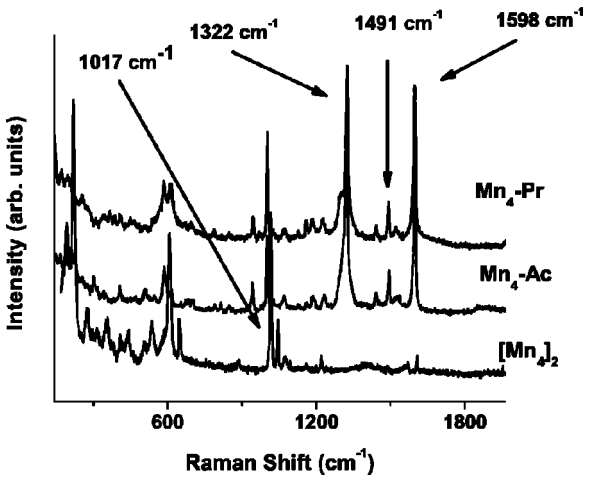

FIG. 4. Spectral comparison of the monomers Mn_4-Pr and Mn_4-Ac with that of the dimer $[Mn_4]_2$. Note the absence from the $[Mn_4]_2$ spectrum of the three ligand vibrations observed in the monomers around 1322, 1491, 1598 cm^{-1}. These are thus assigned to -Pr (O_2CEt) and -Ac (O_2CMe) moieties (see text).

strong peak at 1017 cm^{-1} corresponds to the theoretically predicted value of 1019 cm^{-1}, and is related to vibrations in the pyridine rings. Additionally, the peaks seen in the experiment at 1075, 1222, 1541, 1570, and 1609 cm^{-1} are calculated to appear at 1066, 1207, 1547, 1563, and 1604 cm^{-1}, respectively.

d. O_2CEt vibrations. Peaks which appear at 1044, 1399, 1541, 1570, and 1609 cm^{-1} are assigned to vibrations in the O_2CEt segments of the dimer, as known from the literature.[15] It is worth mentioning that the modes which are located at 1541, 1570, and 1570 cm^{-1} contain contributions from both the -O_2CEt and pyridine components.

The peaks at 810, 1044, 1160, and 1399 cm^{-1} seen in Fig. 2, but not predicted by theory, will be discussed later.

All of the Raman results are summarized in Table I.

B. Use of model compounds for mode assignment

Due to the complexity of the chemical structure of $[Mn_4]_2$, group theoretical techniques were not attempted at this stage for mode assignment. Instead, we took the experimental approach of utilizing a set of model compounds in order to provide additional insight into the peak assignments (Fig. 3). We thus studied the Mn-O bond containing model compounds, MnO_2, $KMnO_4$, and $Mn(O_2CMe)_2$. The mode at 316 cm^{-1} in the SMM, also present in the model compound MnO_2 at 317 cm^{-1}, is due to a Mn-O vibration. The strong peak at 406 cm^{-1} in $KMnO_4$, which is also attributed to Mn-O, matches very well with the mode observed at 409 cm^{-1} in $[Mn_4]_2$. Small broad peaks at 1399, 1570, and 1609 cm^{-1} correspond to the peaks seen in $Mn(O_2CMe)_2$ at 1410, 1572, and 1615 cm^{-1}, which leads to their assignment as relating to Mn-O-*R* vibrations. Additionally, the Raman spectrum of the model compound $MnCl_2$, which contains two peaks at 196 and 281 cm^{-1} was also compared to the $[Mn_4]_2$ data. Due to the similarity of position and intensity to the modes observed at 192 and 274 cm^{-1} in $[Mn_4]_2$, these peaks are assigned to Mn-Cl vibrations.

From literature, the peak observed at 1044 cm^{-1} in the Raman spectrum is assigned to a vibration in O_2CEt.[25] The modes occurring at 1160 and 1609 cm^{-1} are related to vibrations in the pyridine rings.[25]

Raman studies of the related monomers, Mn_4-Pr and Mn_4-Ac, were compared to the spectrum of $[Mn_4]_2$ as seen in Fig. 4. Although the ligand structure is different, the core structure remains identical to that of $[Mn_4]_2$. Several of the peaks in the spectra of Mn_4-Pr and Mn_4-Ac are very similar in both position and magnitude to modes observed in $[Mn_4]_2$. The small peak observed at 192 cm^{-1}, attributed to a Mn-Cl vibration, is evident in both Mn_4-Pr and Mn_4-Ac, at 194 and 191 cm^{-1}, respectively. Because the monomers only contain Mn-Cl in the core cubane, the vibration at 192 cm^{-1} in $[Mn_4]_2$ must be related to Mn-Cl vibrations in the cubane structure. Furthermore, the absence of a Mn-Cl peak at 274 cm^{-1} in the monomers, implies this mode in $[Mn_4]_2$ is related to vibrations in the three Mn-Cl bonds on the periphery of the cubane structure. The intense modes which appear at 1000 and 1029 cm^{-1} in Mn_4-Pr and 1002 and 1027 cm^{-1} in Mn_4-Ac are slightly shifted from analogous peaks seen at 1017 and 1044 cm^{-1} in $[Mn_4]_2$. Although there are many similarities at low frequencies in the spectra of the monomers as compared to the spectrum of the dimer, there are also several striking differences at higher frequencies. This is due to the fact the core cubane vibrations occur at lower frequencies, while the ligand modes appear at a higher range. The most evident of these differences is the absence of the three intense peaks which are observed in the monomers at 1322, 1491, and 1598 cm^{-1}. These vibrations are attributed to the ligands on the monomers which are significantly different than those attached to the dimer. It should also be noted that in the frequency range studied, there do not appear to be any modes which are related specifically to any intermolecular coupling in $[Mn_4]_2$.

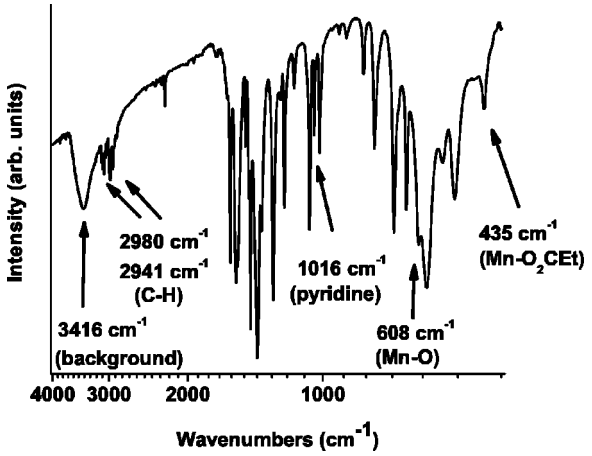

FIG. 5. Typical IR spectrum of the SMM $[Mn_4]_2$. Several of the assigned peaks are noted on the spectrum.

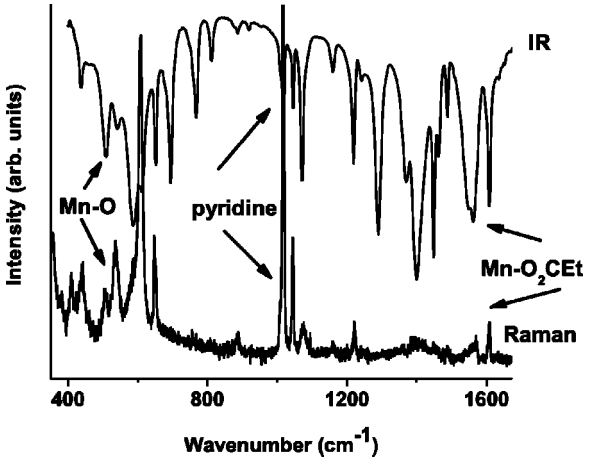

FIG. 6. A comparison of the Raman and IR spectra of $[Mn_4]_2$ shows excellent agreement in the 400–1675 cm^{-1} range.

C. Infrared measurements

The IR spectrum of $[Mn_4]_2$, which can be seen in Fig. 5, contains numerous peaks. Similar to the Raman results, the observed modes are in very good agreement with those predicted by the DFT calculations.[15] A mode related to O^{2-} and Mn, which is calculated to appear at 543 cm^{-1}, is evident in the IR spectrum at 539 cm^{-1}. The peak that is predicted at 1563 cm^{-1} in the theoretical calculations occurs at 1565 cm^{-1} in the IR. This mode is assigned to vibrations in the O_2CEt and the pyridine rings.[15] Peaks observed in the experimental spectrum at 694 and 1161 cm^{-1}, but not predicted by the DFT calculations, are related to pyridine ring vibrations. The mode which appears at 2941 cm^{-1} in the IR, and is predicted at 2942 cm^{-1},[15] is attributed to symmetric C-H vibrations.[25] Additionally, the unpredicted peak at 2980 cm^{-1} is also attributed to an asymmetric C-H vibration.[25] The results of the IR experiments are compared to the Raman results and theoretical calculations in Table I.

It should be noted many of the modes in the IR spectrum also appear in the Raman data. Figure 6 shows a comparison of the spectra from the two techniques. For example, the peak observed at 647 cm^{-1} in the Raman spectrum is also present in the IR at 649 cm^{-1}. The sharp peak at 1609 cm^{-1} in the Raman is observed in the IR at 1608 cm^{-1}, and is predicted by the theory at 1604 cm^{-1}.

D. General remarks on the mode assignments

Due to the large size of $[Mn_4]_2$, there is a collective behavior of the vibrational modes, and thus a breakdown of the traditional selection rules for Raman and IR spectroscopy. We have therefore utilized the ''functional group'' approach for the mode assignment even though the vibrational modes in SMM's (especially the lowest-energy ones) are collective and involve the entire molecule. One significant advantage of the functional group analysis is that the vibrations can be easily visualized and are appropriate for describing the motion of ligands.

IV. CONCLUSIONS

Our goal was to identify the vibrational modes of the dimerized SMM $[Mn_4]_2$. Many of the theoretically predicted Raman modes match well with the experimentally observed spectra. For example, the observed Raman peaks at 192, 219, 274, 316, 354, 382, 409, 443, 509, 537, 608, 647, 1017, 1075, 1222, 1541, 1570, and 1609 cm^{-1} match well with those predicted at 194, 212, 278, 301, 361, 380, 423, 444, 514, 543, 602, 640, 1019, 1066, 1207, 1547, 1563, and 1604 cm^{-1}, respectively.[15] However, peaks at 588, 1044, 1160, and 1399 cm^{-1} are unaccounted for in the theoretical calculations. Additionally, there are several peaks which were predicted that were not observed in the experiment. Through the use of the model compounds, MnO_2, $KMnO_4$, $Mn(O_2CMe)_2$, and $MnCl_2$ and theoretical calculations, several of the previously unaccounted for vibrational modes of the SMM $[Mn_4]_2$ have been assigned. Modes of the monomer compounds Mn_4-Pr and Mn_4-Ac with similar core structures to the dimer have been compared to the spectrum of $[Mn_4]_2$, and help to confirm the mode assignment. Further temperature and magnetic-field-dependent studies are currently in progress. The data provided here suggest the need for further refinement of the theoretical calculations and should elicit additional theoretical and experimental interest in the field of SMM's. They also provide the basis for studies of magnetic-field effects on these modes, as has been reported for Mn_{12}-acetate.[18,19]

ACKNOWLEDGMENTS

We thank the National Science Foundation (NIRT Grant No. DMR 0103290) for financial support. We are grateful to Dr. Kyungwha Park and Dr. Mark Pederson for providing us a preprint of their calculations of the Raman and IR frequencies,[15] and Dr. Bert van de Burgt for help with the Raman measurements.

[1] E.M. Chudnovsky and J. Tejada, *Macroscopic Quantum Tunneling of the Magnetic Moment* (Cambridge University Press, Cambridge, UK, 1998).
[2] G. Christou, D. Gatteschi, and D.N. Hendrickson, MRS Bull. **25**, 66 (2000).
[3] M.N. Leuenberger and D. Loss, Nature (London) **410**, 789 (2001).
[4] T. Lis, Acta Crystallogr., Sect. B: Struct. Crystallogr. Cryst. Chem. **36**, 2042 (1980).
[5] K. Weighardt, K. Pohl, I. Jibril, and G. Huttner, Angew. Chem., Int. Ed. Engl. **23**, 77 (1984).
[6] S.M.J. Aubin, M.W. Wemple, D.M. Adams, H.-L. Tsai, G. Christou, and D.N. Hendrickson, J. Am. Chem. Soc. **118**, 7746 (1996).
[7] S.M.J. Aubin, N.R. Dilley, L. Pardi, J. Krzystek, M.W. Wemple, L.-C. Brunel, M.B. Maple, G. Christou, and D.N. Hendrickson, J. Am. Chem. Soc. **120**, 4991 (1998).
[8] J.R. Friedman, M.P. Sarachik, J. Tejada, and R. Ziolo, Phys. Rev. Lett. **76**, 3830 (1996).
[9] L. Thomas, F. Lionti, R. Ballou, D. Gatteschi, R. Sessoli, and B. Barbara, Nature (London) **383**, 145 (1996).
[10] C. Sangregorio, T. Ohm, C. Paulsen, R. Sessoli, and D. Gatteschi, Phys. Rev. Lett. **78**, 4645 (1997).
[11] J.A.A.J. Perenboom, J.S. Brooks, S. Hill, T. Hathaway, and N.S. Dalal, Phys. Rev. B **58**, 330 (1998).
[12] L. Bokacheva, A.D. Kent, and M.A. Walters, Phys. Rev. Lett. **85**, 4803 (2000).
[13] W. Wernsdorfer, N. Aliaga-Alcalde, D.N. Hendrickson, and G. Christou, Nature (London) **416**, 406 (2002).
[14] S. Hill, R.S. Edwards, N. Aliaga-Alcalde, and G. Christou, Science **302**, 1015 (2003).
[15] K. Park, M.R. Pederson, and N. Bernstein, cond-mat/0307145v1 (unpublished).
[16] K. Park, M.R. Pederson, S.L. Richardson, N. Aiaga-Alcalde, and G. Christou, Phys. Rev. B **68**, 020405(R) (2003).
[17] M.R. Pederson, N. Bernstein, and J. Kortus, Phys. Rev. Lett. **89**, 097202 (2002).
[18] A.B. Sushkov, B. Jones, J.L. Musfeldt, R.M. Achey, and N.S. Dalal, Phys. Rev. B **63**, 214408 (2001).
[19] A.B. Sushkov, J.L. Musfeldt, Y.J. Wang, R.M. Achey, and N.S. Dalal, Phys. Rev. B **66**, 144430 (2002).
[20] J.M. North, L.J. van de Burgt, and N.S. Dalal, Solid State Commun. **123**, 75 (2002).
[21] J.M. North, R.M. Achey, and N.S. Dalal, Phys. Rev. B **66**, 174437 (2002).
[22] J.M. North and N.S. Dalal, J. Appl. Phys. **93**, 7092 (2003).
[23] (a) J.B. Vincent, H.R. Chang, K. Folting, J.C. Huffman, G. Christou, and D.N. Hendrickson, J. Am. Chem. Soc. **109**, 5703 (1987); (b) M.W. Wemple, H.-L. Tsai, K. Folting, D.N. Hendrickson, and G. Christou, Inorg. Chem. **32**, 2025 (1993).
[24] D.N. Hendrickson, G. Christou, E.A. Schmitt, E. Libby, J.S. Brashkin, S. Wang, H.-L. Tsai, J.B. Vincent, P.D.W. Boyd, J.C. Huffman, K. Folting, Q. Li, and W.E. Streib, J. Am. Chem. Soc. **114**, 2455 (1992).
[25] D.L. Pavia, G.M. Lampman, and G.S. Kriz, *Introduction to Spectroscopy* (Saunders, New York, NY, 1997).